

## Organic Cation Transport in Rabbit Alveolar Epithelial Cell Monolayers

Jie Shen,<sup>1</sup> Katharina J. Elbert,<sup>1,2,3</sup>  
Fumiyoshi Yamashita,<sup>4</sup> Claus-Michael Lehr,<sup>3</sup>  
Kwang-Jin Kim,<sup>5</sup> and Vincent H. L. Lee.<sup>1,6,7</sup>

Received March 22, 1999; accepted May 11, 1999

**Purpose.** To characterize organic cation (OC) transport in primary cultured rabbit alveolar epithelial cell monolayers, using [<sup>14</sup>C]-guanidine as a model substrate.

**Methods.** Type II alveolar epithelial cells from the rabbit lung were isolated by elastase digestion and cultured on permeable filters pre-coated with fibronectin and collagen. Uptake and transport studies of [<sup>14</sup>C]-guanidine were conducted in cell monolayers of 5 to 6 days in culture.

**Results.** The cultured alveolar epithelial cell monolayers exhibited the characteristics of a tight barrier. [<sup>14</sup>C]-Guanidine uptake was temperature dependent, saturable, and inhibited by OC compounds such as amiloride, cimetidine, clonidine, procainamide, propranolol, tetraethylammonium, and verapamil. Apical guanidine uptake ( $K_m = 129 \pm 41 \mu\text{M}$ ,  $V_{\max} = 718 \pm 72 \text{ pmol/mg protein/5 min}$ ) was kinetically different from basolateral uptake ( $K_m = 580 \pm 125 \mu\text{M}$ ,  $V_{\max} = 1,600 \pm 160 \text{ pmol/mg protein/5 min}$ ). [<sup>14</sup>C]-Guanidine transport across the alveolar epithelial cell monolayer in the apical to basolateral direction revealed a permeability coefficient ( $P_{app}$ ) of  $(7.3 \pm 0.4) \times 10^{-7} \text{ cm/sec}$ , about seven times higher than that for the paracellular marker [<sup>14</sup>C]-mannitol. **Conclusions.** Our findings are consistent with the existence of carrier-mediated OC transport in cultured rabbit alveolar epithelial cells.

**KEY WORDS:** alveolar epithelial cell monolayers; organic cation transport; guanidine.

### INTRODUCTION

There is growing interest in drug delivery via the pulmonary route. Three models have been used to study pulmonary drug transport: *in vivo* animal model, isolated and perfused whole lung model, and *in vitro* cell culture model. Compared to the other two, *in vitro* cultures of distal lung epithelial cells

eliminate the inherent problems associated with a complex anatomical structure of the lung, and provide direct information on the permeability of the distal lung epithelial lining. Previous work based on primary cultured rat alveolar epithelial cell monolayers revealed passive diffusional transport mechanisms for lipophilic drugs such as beta adrenergic antagonists (1), paracellular transport mechanism for hydrophilic solutes such as thyrotropin-releasing hormone (2), and carrier-mediated mechanism for dipeptides such as Gly-L-Phe (3).

Lung tissue is also known to accumulate a variety of organic cations both *in vivo* and *in vitro*. Both repair of the injured lung (4) and compensatory growth of the remaining tissue after partial resection (5) are initiated by enhanced synthesis and uptake of amines due to their important roles in a number of cellular processes. Active accumulation of organic cations in alveolar epithelial type I and type II cells has been demonstrated previously in rabbit lung slices (6).

A large number of drugs exist as organic cations (OC) at physiological pH. They include anticholinergic, adrenergic, antineoplastic, anesthetic, sympathomimetic, and antihistaminic drugs. Among these,  $\beta$ -adrenergic agonists like metaproterenol and fenoterol have been used via inhalation to treat asthma (7). Blood-borne OC drugs like amphetamine, imipramine, and chlorpromazine are known to be filtered out of the blood and retained in the lung (8). Understanding the mechanism of OC transport in the lung epithelial cells should therefore be beneficial from a drug delivery point of view, either to guide airborne OC drugs across the alveolar epithelium for systemic delivery, or to direct blood-borne OC drugs to the lung for local action.

Carrier-mediated OC transport in epithelial cells has been demonstrated in the kidneys (for tubular secretion) (9,10). Studies using isolated kidney proximal tubule plasma membrane vesicles have revealed basolateral uptake of OCs via a carrier-mediated system that is driven by a membrane potential difference (9), followed by secretion via OC/H<sup>+</sup> exchange at the brush border membrane (10). Similar mechanisms for OC transport are also observed in the liver (11), responsible for hepatobiliary excretion. Epithelial OC transport is also present in the choroid plexus (for absorption) (12), placenta (for excretion) (13), and small intestine (for absorption and secretion) (14).

The purpose of the present study was to determine whether alveolar epithelial cells transport OC compounds, using the primary cultured rabbit alveolar epithelial cell monolayers as a model. As already mentioned, alveolar epithelial cell culture has been previously established with rat pneumocytes (15) and used in ion and drug transport studies (16). In our study, typically 75–100 million purified alveolar type II cells can be harvested from one rabbit, in contrast to yields of 10 million such cells per rat (15). The advantage of using rabbit over rat as a source of alveolar epithelial cells is therefore obviation of the experimental complexity of harvesting cells from several animal lungs simultaneously, thereby significantly reducing the number of animals required. In addition, the isolated and perfused rabbit lung has been used as a model in many drug pharmacokinetic studies, the results of which may serve as a reference for correlation of the transport data obtained from cultured rabbit alveolar epithelial cells. Following establishment of the culture model, OC uptake and transport studies were conducted in the alveolar epithelial cell monolayers.

<sup>1</sup> Department of Pharmaceutical Sciences, University of Southern California, Los Angeles, California 90033.

<sup>2</sup> Present address: Advanced Inhalation Research, Inc., Cambridge, Massachusetts 02139.

<sup>3</sup> Department of Biopharmaceutics and Pharmaceutical Technology, Saarland University, Saarbrücken, Germany.

<sup>4</sup> Department of Drug Delivery Research, Kyoto University, Kyoto, Japan.

<sup>5</sup> Departments of Medicine, Physiology and Biophysics, Molecular Pharmacology and Toxicology, Biomedical Engineering, and Will Rogers Institute Pulmonary Research Center, University of Southern California, Los Angeles, California 90033.

<sup>6</sup> Department of Ophthalmology, University of Southern California, Los Angeles, California 90033.

<sup>7</sup> To whom correspondence should be addressed at School of Pharmacy, Department of Pharmaceutical Sciences, PSC 704, University of Southern California, 1985 Zonal Avenue, Los Angeles, California 90033. (e-mail: vincentl@hsc.usc.edu)

[<sup>14</sup>C]Guanidine, a primary amine which exists almost exclusively as the positively charged guanidinium ion at physiological pH ( $pK_a = 12.5$ ), was selected as a model compound to characterize OC uptake in primary cultured rabbit alveolar epithelial cell monolayers with respect to temperature dependency, saturability, and competition with other OCs. [<sup>14</sup>C]Guanidine has been used to characterize organic cation transport in the human kidney (10).

## MATERIALS AND METHODS

### Materials

Male, New Zealand, albino rabbits (1–1.3 kg) were obtained from Irish Farm (Los Angeles, CA). The investigations utilizing rabbits described in this report conformed to the Guiding Principles in the Care and Use of Animals (DHEW Publication, NIH 80-23). Heparin (sodium injection, USP, 5000 U/ml) was purchased from Elkins-Sinn, Inc. (Cherry Hill, NJ). Dulbecco's modified Eagle's medium nutrient mixture F-12 Ham (DMEM/F12), minimum essential Eagle's medium, lectin from *Bandeiraea simplicifolia* BS-I, deoxyribonuclease I (type IV, DNase I), trypsin inhibitor (type II-S: soybean), human recombinant epidermal growth factor (EGF), hydrocortisone and bovine serum albumin (BSA) were purchased from Sigma (St. Louis, MO). Fetal bovine serum (FBS), Fungizone™, penicillin-streptomycin, L-glutamine, and gentamicin were purchased from Life Technologies (Grand Island, NY). Non-coated clear Transwells™ and Snapwells™ were obtained from Costar (Cambridge, MA). ITS+ Premix (culture supplement containing insulin, transferrin, selenium, linoleic acid, and BSA), recombinant human fibronectin, and type I rat tail collagen were obtained from Collaborative Biomedical Products (Bedford, MA). Porcine pancreatic elastase was from Worthington Biochemical Corporation (Freehold, NJ).

### Primary Culture of Alveolar Epithelial Cell Layers

#### Isolation of Alveolar Type II Cells

Alveolar type II cells were isolated from the rabbit lung using a method modified from that described by Mason *et al.* (17). Briefly, animals were first injected with ~1.5 ml heparin (1 ml/kg) and then euthanized by a rapid injection of 1.5 mg sodium pentobarbital solution/kg, both via a marginal ear vein. The abdominal cavity was opened. The lung was ventilated manually by tracheal cannulation with a 60 ml syringe and the lung blood circulation was perfused with PBS (1 mM KH<sub>2</sub>PO<sub>4</sub>, 155 mM NaCl, and 3 mM Na<sub>2</sub>HPO<sub>4</sub>) via the pulmonary vein. After the lung was lavaged several times with PBS containing 3 mM EDTA and once with DMEM/F12 containing 2 U/ml elastase, about 40 ml of a 2 U/ml elastase solution was instilled through the trachea and the lung was incubated at 37°C for a total of 35 min.

The lung was excised from the trachea and the bronchi, and transferred to a DMEM/F12 solution containing 1.67 mg/ml trypsin inhibitor. The lung pieces were minced and transferred to a sterilized Erlenmeyer flask. The lung tissue suspension was sequentially filtered through gauze, a 40 μm cell strainer, and a 15 μm nylon mesh. The cell suspension was centrifuged at 200 × g for 8 min at 4°C. The cell pellets were resuspended

in DMEM/F12. The crude cell suspension was incubated with 16 μg/ml BS-I lectin, as described by Simon *et al.* (18), at room temperature for 30 min and subsequently filtered through 40 μm cell strainers. The filtered cell suspension was centrifuged and the cell pellet was resuspended in DMEM/F12 containing 10% FBS. Cell viability was estimated to be 91 ± 3% (n = 15) by the trypan blue dye exclusion method.

#### Culture Conditions

Purified type II cells were plated onto Costar 6.5 mm Transwells™ or 12 mm Snapwells™ inserts (precoated with 30 μg/ml Type I collagen plus 10 μg/ml fibronectin) at various cell counts per unit volume to determine the optimum seeding density. The cells were plated in DMEM/F12 containing 10% FBS and 2 mM L-glutamine for the first two days of culture. In order to inhibit the growth of fibroblasts, the medium was changed to serum-free DMEM/F12 supplemented with ITS+, 2.0 mM L-glutamine, 10 ng/ml EGF and 1 μM hydrocortisone. The cultures were fed every other day with a serum-free defined medium. Cultures were maintained in a humidified 5% CO<sub>2</sub> incubator at 37°C. Beginning on day 3 in culture, transepithelial electrical resistance (TEER, kΩ) and spontaneous potential difference (PD, mV) were measured with an EVOM device (World Precision Instruments, Sarasota, FL). Correction was made for solution resistance (~100 Ω) using a blank filter.

#### Purity Check

To assess the purity of the isolated alveolar epithelial cells, tannic acid staining, which targets the lamellar inclusion bodies of type II cells, was performed, as described by Mason *et al.* (17). Briefly, freshly isolated type II cells were either spun down onto microscope slides or plated on tissue culture-treated chamber slides and maintained in the same way as cells plated on the filter support. The cells were fixed by glutaraldehyde and osmium tetroxide, and stained by tannic acid overnight. The purity of the type II cells, as measured by counting cells that were stained versus the total cell population, was estimated to be (89 ± 5)% (n = 5).

In addition to tannic acid staining, alkaline phosphatase staining was performed, as described by Edelson *et al.* (19), to assess the number of macrophage cells, the major contaminating cell type in alveolar cell isolation. Alveolar type II cells are known to be alkaline phosphatase positive, while macrophages stain negative for the enzyme (19). Briefly, freshly isolated cell suspension was spun down onto glass slides and air-dried. Cells were then stained with naphthol As-B1 phosphate and fast red reagent. Hematoxylin was used to counterstain the slides. Macrophage contamination was estimated to be (7 ± 2)% (n = 4).

### Ion Transport Activity of Primary Cultured Alveolar Epithelial Cell Monolayers

Cell monolayers were grown on Snapwell™ filters and mounted in modified Ussing chambers for the assessment of bioelectric properties, as described by Robison and Kim (20). Cell monolayers were bathed on both sides with an identical bicarbonated Ringer's solution at 37°C. The Ringer's solution contained 116.4 mM NaCl, 5.4 mM KCl, 1.8 mM CaCl<sub>2</sub>, 0.81 mM MgSO<sub>4</sub>, 0.78 mM NaH<sub>2</sub>PO<sub>4</sub>, 25 mM NaHCO<sub>3</sub>, 15 mM HEPES, and 5 mM D-glucose. A stream of 5% CO<sub>2</sub> in air was

continuously blown across the surfaces of the bathing fluids to maintain constant pH. To demonstrate the presence of active ion transport in the alveolar epithelial cells, the effect of ion transport inhibitors (10  $\mu$ M apical amiloride and 0.5 mM basolateral ouabain) and an apical Na<sup>+</sup>-free condition on the short-circuit current ( $I_{sc}$ ) of cell monolayers was monitored. The monolayers were allowed to attain a steady-state  $I_{sc}$  prior to the addition of a pharmacological agent to the bathing solution or superfusion of Na<sup>+</sup>-free buffer on the apical side.

### Transepithelial Solute Transport Across Cultured Alveolar Epithelial Cell Monolayers

To assess the paracellular permeability barrier property of the alveolar epithelial cell monolayer, [<sup>3</sup>H]-mannitol transport across the cell monolayer was measured. Briefly, a total of 100  $\mu$ l of 5  $\mu$ Ci/ml [<sup>3</sup>H]-mannitol was applied to the apical side of the cell monolayer, while the basolateral side was bathed in pH 7.4 bicarbonated Ringer's solution. At 0.5, 1, 1.5, 2, 2.5, 3, 3.5, and 4 hr, a 100  $\mu$ l aliquot was taken from the basolateral compartment, mixed with 5 ml scintillation cocktail (Econosafe, Research Products International, Mount Prospect, IL), and counted for radioactivity in a liquid scintillation counter. The basolateral volume was replenished with 100  $\mu$ l fresh buffer after each sampling. [<sup>14</sup>C]-Guanidine (2.75  $\mu$ Ci/ml) transport was conducted in a similar way.

The apparent permeability (cm/sec) of the solutes was determined from the following relationship:  $P_{app} = J/(A \cdot C)$ , where  $J$  (pmol/sec) is the transport rate,  $A$  (cm<sup>2</sup>) is the filter surface area, and  $C$  (nM) is the initial dosing concentration. Data were compared using the unpaired t-test, and  $p < 0.01$  was considered as statistically significant.

### [<sup>14</sup>C]-Guanidine Uptake

Cellular uptake at 50  $\mu$ M donor concentration of [<sup>14</sup>C]-guanidine was studied with cells grown on permeable Transwell™ filters for 5 to 6 days. Cells were always bathed in pH 7.4 bicarbonated Ringer's solution on the receiver side. In preliminary studies, uptake at 37°C was found to be linear for up to 5 min. Therefore, 5 min was chosen as the sampling time point for subsequent experiments.

The kinetic parameters of guanidine uptake by alveolar epithelial cells were determined by measuring uptake as a function of substrate concentration (0.01–1 mM), both at the apical and basolateral membrane of the cell monolayers. In inhibition experiments, 5 mM of various compounds (except for amiloride and verapamil, which were used at 1 mM for solubility reason) were co-incubated for five minutes with [<sup>14</sup>C]guanidine in cells. Uptake was terminated by aspirating the dosing solution and rinsing the cell monolayers six times in ice-cold PBS buffer (pH 7.4). The cell monolayers were then cut out from the Transwell™ and immersed in 0.5 ml of 0.1% Triton X-100 to lyse the cells. After overnight incubation at room temperature and subsequent vigorous vortexing, 20  $\mu$ l of cell lysate was taken from each sample for protein assay (DC protein kit, Bio-Rad Laboratories, Hercules, CA) to normalize uptake data. The radioactivity in the cell lysate was determined as described in the transport experiments. Bare Transwell™ filters with no cells seeded on them served to assess nonspecific binding of [<sup>14</sup>C]-guanidine (~2% of total cpm) for correction of the cellular uptake data.

The guanidine uptake vs. concentration data were fitted to the relationship:

$$\text{Uptake} = (V_{\max} \cdot C)/(K_m + C) + K_d \cdot C$$

where  $V_{\max}$  is the maximal transport rate,  $K_m$  is the half-maximal guanidine concentration, and  $C$  is the guanidine concentration in the dosing solution. The nonsaturable component,  $K_d$ , of the uptake rate was determined by estimating the slope of linear guanidine uptake in the presence of 5 mM inhibitor clonidine. Clonidine was used as an inhibitor for the saturable process, since it showed the most potent inhibition in guanidine uptake (Fig. 7)

## RESULTS

### Primary Cultured Rabbit Alveolar Epithelial Cells

We first evaluated the effect of seeding density on the development of the alveolar epithelial cell monolayers. As shown in Table I, seeding densities of either 0.33 or 0.44  $\times 10^6$  cells/cm<sup>2</sup> did not yield appreciable TEER or PD values, whereas other densities led to peak TEER values of exceeding 1 k $\Omega$ ·cm<sup>2</sup> and peak PD values exceeding 10 mV (apical side as reference). These data suggest that 0.88 and 1.33  $\times 10^6$  cells/cm<sup>2</sup> were the optimum seeding densities for the primary culture of rabbit alveolar epithelial cells. We chose 0.88  $\times 10^6$  cells/cm<sup>2</sup> as the seeding density for all other studies. As shown in Fig. 1, both TEER and PD peaked by day 6 at 1.98  $\pm$  0.02 k $\Omega$ ·cm<sup>2</sup> and 34.5  $\pm$  0.8 mV, respectively ( $n = 60$ ).

### Morphological Observations

As shown in Fig. 2, rabbit alveolar cells in culture changed over time in morphology, appearing as spread-out cytoplasmic projections with a concomitant loss of their characteristic lamellar inclusion bodies.

### Active Na<sup>+</sup> Transport in Cultured Alveolar Epithelial Cell Monolayers

Figure 3 summarizes the effect of apical amiloride, basolateral ouabain, and apical Na<sup>+</sup>-free condition on  $I_{sc}$  and TEER in cultured alveolar epithelial cell monolayers. Addition of the Na<sup>+</sup>,K<sup>+</sup>-ATPase inhibitor ouabain (0.5 mM) to the basolateral fluid induced a gradual decrease in  $I_{sc}$  to less than 5% of its initial value at 35 min, while not changing the TEER significantly (Fig. 3A). Addition of the Na<sup>+</sup> channel blocker amiloride (10  $\mu$ M)

**Table I.** Effect of Seeding Density on the Development of Peak Bioelectric Parameters in Rabbit Alveolar Epithelial Cell Culture (mean  $\pm$  s.e.m.,  $n = 4-7$ )

Seeding density ( $\times 10^6$ cells/cm <sup>2</sup> )	TEER (k $\Omega$ ·cm <sup>2</sup> )	PD (mV)	Day of peak bioelectric performance
0.33	0.23 $\pm$ 0.06	3.5 $\pm$ 0.2	7.0 $\pm$ 0.2
0.44	0.90 $\pm$ 0.4	4.0 $\pm$ 0.4	6.1 $\pm$ 0.6
0.67	1.8 $\pm$ 0.1	11 $\pm$ 1	6.5 $\pm$ 0.1
0.88	2.0 $\pm$ 0.1	34 $\pm$ 2	6.2 $\pm$ 0.1
1.33	1.8 $\pm$ 0.2	20 $\pm$ 5	6.0 $\pm$ 0.2

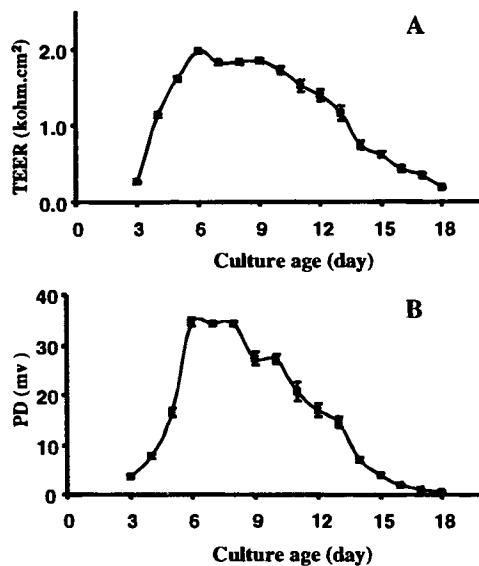
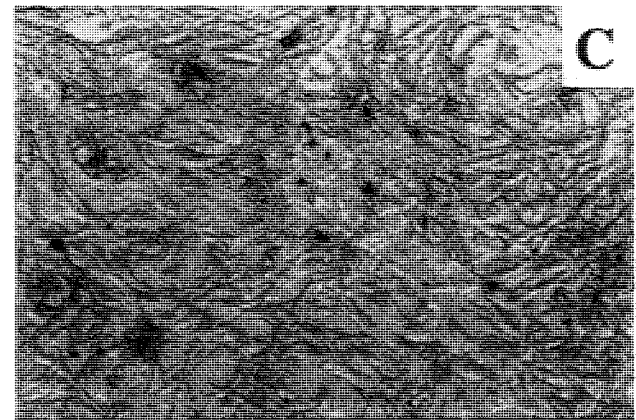
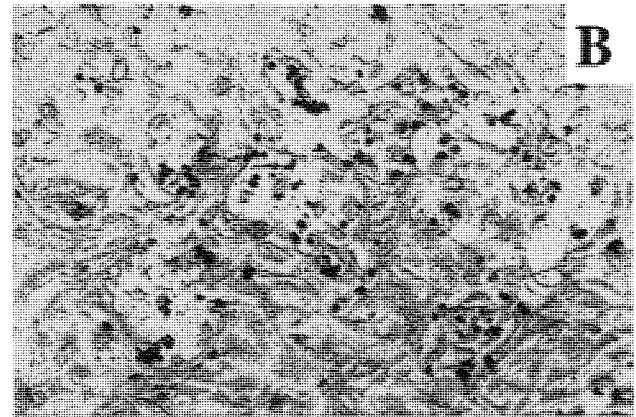
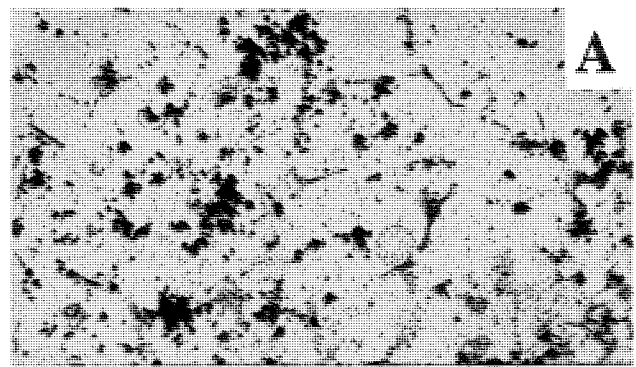


**Fig. 1.** Time course of transepithelial electrical resistance (TEER, panel A) and potential difference (PD, panel B) of cultured primary rabbit alveolar epithelial monolayers, seeded at  $0.88 \times 10^6$  cells/cm<sup>2</sup>. Each data point represent mean  $\pm$  s.e.m. for  $n = 60$  from 10 different preparations.



to the apical side inhibited  $I_{sc}$  by  $\sim 50\%$  (Fig. 3B). Superfusion of Na<sup>+</sup>-free buffer to the apical fluid rapidly abolished  $I_{sc}$  within 10 min (Fig. 3C), while replenishment of Na<sup>+</sup> led to a recovery in  $I_{sc}$  to 80% of its initial value.

#### Permeability of Cell Monolayers to Mannitol and Guanidine

The fluxes of the paracellular marker [<sup>3</sup>H]-mannitol (5  $\mu$ Ci/ml) and [<sup>14</sup>C]-guanidine (50  $\mu$ M, 27.5  $\mu$ Ci/ml) across the alveolar epithelial cell monolayer from the apical to basolateral side are shown in Fig. 4. A lag time of 0.5 hr was observed for guanidine flux, but not for mannitol flux. The  $P_{app}$  of [<sup>3</sup>H]-mannitol was  $(1.01 \pm 0.03) \times 10^{-7}$  cm/sec ( $n = 4$ ), while that of guanidine was  $(7.20 \pm 0.87) \times 10^{-7}$  cm/sec ( $n = 6$ ).

#### Guanidine Uptake

##### Temperature Dependency

Both apical (Panel A) and basolateral (Panel B) uptake of [<sup>14</sup>C]-guanidine into alveolar epithelial cells showed temperature dependency (Fig. 5). At 37°C, uptake from apical fluid within 30 min was slightly lower than that from basolateral fluid. At 4°C, both uptake processes were significantly lower (by 50 to 60%) than that at 37°C at all time points.

##### Kinetics

As seen in Figs. 6A and 6B, both apical and basolateral uptake processes consist of both a saturable and a non-saturable component. The saturable component (denoted by a dashed line in the figures) was calculated by subtracting the linear non-saturable component from total uptake, and was used to estimate the kinetic parameters of guanidine

uptake. Panel A, day 2. Most cells retained their lamellar inclusion bodies. Panel B, day 4. Fewer cells were stained compared to those on day 2 and many cells started to spread out with thin cytoplasmic projections. Panel C, day 6. Very few cells were stained as the monolayer became confluent.

uptake. For apical uptake,  $K_m$  was  $129 \pm 41$   $\mu$ M and  $V_{max}$  was  $718 \pm 72$  pmol/mg protein/5 min. For basolateral uptake, these constants were  $580 \pm 125$   $\mu$ M and  $1,600 \pm 160$  pmol/mg protein/5 min, respectively. The non-saturable component showed a  $K_d$  value of  $0.45 \pm 0.05$  and of  $0.22 \pm 0.01$  pmol/ $\mu$ M/mg protein/5 min ( $P < 0.01$ ), for apical and basolateral uptake, respectively.

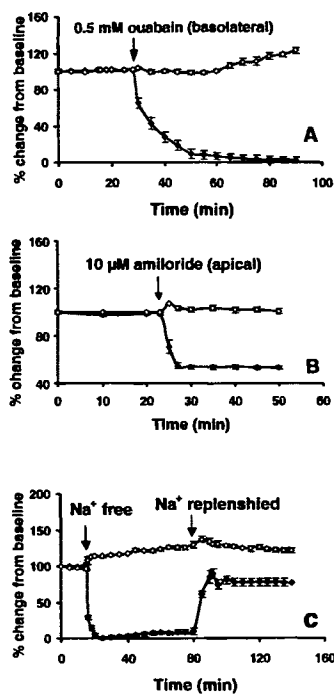


**Fig. 3.** Effects of basolateral 0.5 mM ouabain (Panel A), apical 10  $\mu$ M amiloride (Panel B), and apical  $Na^+$ -free condition (Panel C) on baseline short-circuit current ( $I_{sc}$ ,  $\blacklozenge$ ) and transepithelial electrical resistance (TEER,  $\circ$ ) of cultured rabbit alveolar epithelial monolayers. Data represent mean  $\pm$  s.e.m. for  $n = 3-5$ .

#### Inhibition

Apical and basolateral uptake of [ $^{14}C$ ]guanidine by alveolar epithelial cells were inhibited by the OC compounds by 50–88% ( $p < 0.001$ ), including amiloride, cimetidine, clonidine, guanidine, procainamide, propranolol, tetraethylammonium (TEA), and verapamil (Fig. 7). Acyclovir, a nucleoside analog, zwitterionic cephalixin, and p-aminohippuric acid (PAH), an organic anion compound, had no significant effect on either apical or basolateral uptake of [ $^{14}C$ ]guanidine by rabbit alveolar epithelial cells.

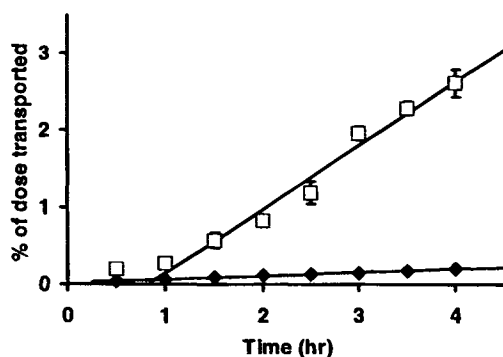


**Fig. 4.** Time course of guanidine ( $\square$ ) and mannitol transport ( $\blacklozenge$ ) across the cultured rabbit alveolar epithelial cell monolayer in the apical to basolateral direction. Each data point represents mean  $\pm$  s.e.m. for  $n = 6$ . Error bars are smaller than the symbols when not seen.

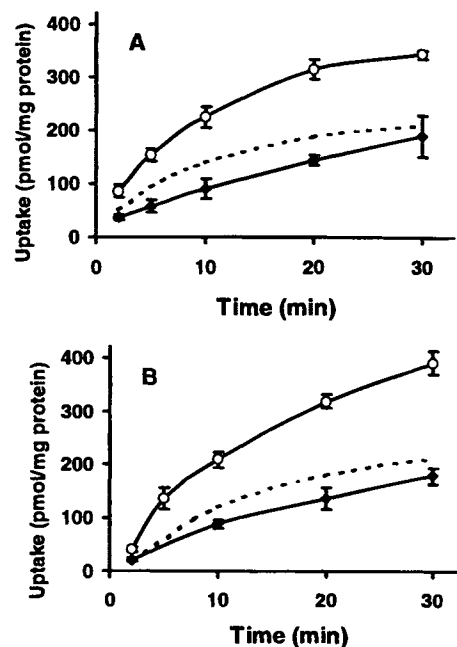


**Fig. 5.** Time course of guanidine uptake by cultured alveolar epithelial cell monolayer from the apical (Panel A) and basolateral fluid (Panel B). Each data point represents the mean  $\pm$  s.e.m. for  $n = 4$ . Key:  $\circ$ , 37°C;  $\blacklozenge$ , 4°C. The dashed line represents the difference in uptake between the two temperatures.

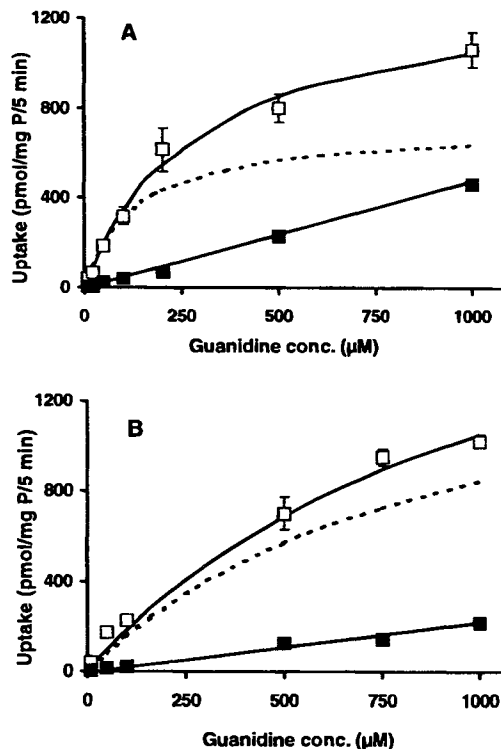


**Fig. 6.** [ $^{14}C$ ]-Guanidine uptake (at 5 min) by rabbit alveolar epithelial cells from the apical (Panel A) and basolateral fluid (Panel B), respectively, as a function of dosing concentration, in the presence and absence of 5 mM clonidine. The dashed line represents the difference in uptake caused by the inhibitor. Each data point represents mean  $\pm$  s.e.m. of 5 samples. Error bars when not seen are smaller than the symbols. Keys:  $\square$ , total uptake;  $\blacksquare$ , uptake in the presence of 5 mM clonidine.

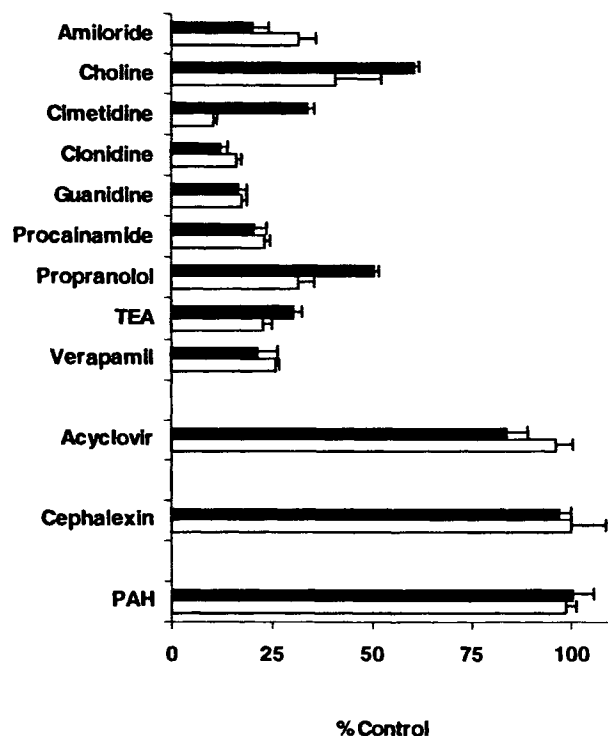


Fig. 7. Apical (■) and basolateral (□) uptake of 50  $\mu$ M [ $^{14}$ C]-guanidine in rabbit alveolar epithelial cells in the presence and absence of various compounds (5 mM except for amiloride and verapamil at 1 mM), at pH 7.4. Data represent mean  $\pm$  s.e.m. for  $n = 5$ . All organic cations, including amiloride, cimetidine, clonidine, guanidine, procainamide, propranolol, tetraethylammonium (TEA), and verapamil, inhibited [ $^{14}$ C]-guanidine uptake significantly ( $p < 0.001$  by ANOVA). Acyclovir, cephalixin, and PAH exerted no inhibition.

## DISCUSSION

OC transport activities have been reported in many organs, including kidney, intestine, liver, brain, and placenta (13,21). Here, we reported the possible existence of carrier-mediated OC transport in primary cultured rabbit alveolar epithelial cell monolayers.

### Development and Characterization of A Primary Cell Culture Model of Rabbit Alveolar Epithelial Cells

We have developed a primary cultured rabbit alveolar epithelial cell model that exhibits characteristics similar to those in the rat alveolar epithelial cell culture model (15). These characteristics include morphological features, exhibition of active ion transport activities, and formation of a tight epithelium.

Isolation of rabbit alveolar epithelial cells for culture on a permeable support differs from that of the rat cells in its purification method. Rabbit alveolar cells were purified effectively by *Griffonia simplicifolia* I lectin, which agglutinates both red blood cells and macrophages (18). By contrast, the rat alveolar cells were purified either by a discontinuous metrizamide gradient (15) or by panning the cell suspension on bacteriologic plates coated with nonspecific IgG (3). Following

isolation, however, rabbit alveolar cells were cultured on a permeable support under similar conditions as for rat alveolar epithelial cells, albeit at a lower seeding density ( $0.88 \times 10^6$  vs.  $1.26 \times 10^6$  cells/cm $^2$ ) (3). Morphologically, rabbit alveolar epithelial cells changed drastically as they aged in culture (Fig. 2). Cells during early stage of the culture were small and contained a large number of lamellar bodies characteristic of alveolar Type II cells (Fig. 2A, tannic acid-stained cells). Over time, they spread out, lost their lamellar bodies, and became confluent (Fig. 2B and 2C). Similar morphological observations were reported for cultured rat type II pneumocytes (22).

In terms of bioelectric properties, TEER of the rabbit alveolar epithelial cell monolayers reached  $1.98 \pm 0.02$  k $\Omega$ ·cm $^2$ , comparable to the value of  $2.26 \pm 0.11$  k $\Omega$ ·cm $^2$  in the rat (15). The peak PD value, however, was more than three-times higher than that in the rat alveolar epithelial cell monolayers ( $34.5 \pm 0.8$  vs.  $9.7 \pm 0.72$  mV) (15), suggesting a more robust active ion transport process in the rabbit alveolar epithelial cell monolayer. A recent study using cultured human alveolar epithelial cells reported bioelectric parameters of TEER =  $2.18 \pm 0.62$  k $\Omega$ ·cm $^2$  and PD =  $13.5 \pm 1.0$  mV (23). Active absorption of Na $^+$  in the apical to basolateral direction across the distal respiratory epithelium is the mechanism for removal of alveolar airspace fluid *in vivo* (24). In our cultured rabbit alveolar epithelial cell monolayers, the apical Na $^+$ -free condition led to complete inhibition of active ion transport (Fig. 3C). This suggests that active Na $^+$  absorption accounts for most, if not all, of active ion transport, about 50% of which is sensitive to amiloride (Fig. 3B). The balance of active ion transport may include Cl $^-$  secretion (25) and amiloride-insensitive Na $^+$  absorption. In the case of cultured rat alveolar epithelial cell monolayers, 80% of the  $I_{sc}$  is contributed by apical amiloride-sensitive Na $^+$  absorption (15).

An important function of the alveolar epithelial barrier is to restrict the movement of water and solutes by maintaining tight intercellular junctions. The apparent permeability of the paracellular marker mannitol in the cultured rabbit alveolar cell monolayer was  $1.01 \times 10^{-7}$  cm/sec, comparable to the value of  $1.80 \times 10^{-7}$  cm/sec found in cultured rat alveolar epithelial cell monolayers (26) and not very different from the value of  $0.45 \times 10^{-7}$  cm/sec estimated in rat alveolar epithelium *in vivo* (16).

In summary, the primary cultured rabbit alveolar epithelial cell monolayers exhibit both active ion transport activities and restricted diffusion of solutes, making them suitable for drug transport and uptake studies.

### OC Transport Activity in Cultured Rabbit Alveolar Epithelial Cells

We have obtained evidence for the existence of carrier-mediated OC transport in primary cultured rabbit alveolar epithelial cells. Guanidine transport across the alveolar epithelial cell monolayer in the apical to basolateral direction was seven times greater than that of mannitol transport. Since guanidine is very hydrophilic and therefore does not freely diffuse across the lipid cell membrane, such a high guanidine permeability is probably the result of carrier-mediated transcellular transport. This process is specific for organic cations, since apical [ $^{14}$ C]-guanidine uptake was significantly inhibited by only organic cations (Fig. 7).

In our study, saturable guanidine transport was observed at both the apical and the basolateral membranes of the rabbit alveolar epithelial cells (Fig. 6). The  $K_m$  value for guanidine uptake was about four times lower for apical than basolateral uptake, while the apical  $V_{max}$  value was about half of that for basolateral uptake. This suggests the possible existence of two distinct OC transport mechanisms in the apical and basolateral plasma membranes of rabbit alveolar epithelial cells, with apical guanidine uptake being of higher affinity but lower capacity. Other OC transport studies using epithelial membrane vesicles have also revealed different profiles for apical versus basolateral transport (27–29).

A thorough understanding of carrier-mediated transport processes across the distal lung epithelium would facilitate the development of new pulmonary drug delivery strategies. Since many drug molecules are positively charged at physiological pH, characterization of the OC transporters in the alveolar epithelial cells would also facilitate the design of OC drugs with exquisite affinity for the OC transporter system.

In addition to its physiological and pharmacological significance, the OC transport process may also bear toxicological significance. For instance, paraquat (1,1'-dimethyl-4,4'-bipyridylum dichloride), a contact herbicide and itself an OC, is highly toxic to the lung, causing severe anoxia and even death. This has been attributed to paraquat accumulation in the alveolar epithelial cells by a process known to take up endogenous diamines and polyamines (30). Inhaled addictive drugs such as heroin and nicotine, being OC compounds, may be absorbed across the alveolar epithelial cell layers via the OC transport processes. Therefore, elucidation of the OC transport mechanism may facilitate the development of strategies to dampen the toxicological consequence just mentioned.

In summary, a primary culture of rabbit alveolar epithelial cell monolayer has been established for drug uptake and transport studies. There exist kinetically distinct carrier-mediated processes for accumulating OC compounds on the apical and basolateral sides of primary cultured rabbit alveolar epithelial cells. Work is underway to elucidate the driving force for OC transport in such a model system.

## ACKNOWLEDGMENTS

Supported in part by the National Institutes of Health grants GM53128 (VHLL), HL38658(KJK), HL46943(KJK), DAAD (KJE), and NATO CRG950302(CML).

## REFERENCES

- P. Saha, K. J. Kim, and V. H. L. Lee. Influence of lipophilicity on  $\beta$ -blocker transport across rat alveolar epithelial cell monolayers. *J. Contr. Rel.* **32**:191–200 (1994).
- K. Morimoto, H. Yamahara, V. H. L. Lee, and K. J. Kim. Transport of thyrotropin-releasing hormone across rat alveolar epithelial cell monolayers. *Lab. Invest.* **54**:2083–2092 (1994).
- K. Morimoto, H. Yamahara, V. H. L. Lee, and K. J. Kim. Dipeptide transport across rat alveolar epithelial cell monolayers. *Pharm. Res.* **10**:1668–1674 (1993).
- A. D. Hacker, D. F. Tierney, and T. K. O'Brien. Polyamine metabolism in rat lungs with oxygen toxicity. *Biochem. Biophys. Res. Commun.* **113**:491–496 (1983).
- D. E. Rannels, J. L. Addison, and R. A. Bennet. Increased pulmonary uptake of exogenous polyamines after unilateral pneumonectomy. *Am. J. Physiol.* **250**:E435–E440 (1986).
- N. A. Saunders, P. J. Rigby, K. F. Ilett, and R. F. Minchin. Autoradiographic localization of putrescine uptake to Type II pneumocytes of rabbit lung slices. *Lab. Invest.* **59**:380–386 (1988).
- R. Beasley, S. Nishima, N. Pearce, and J. Crane. Beta-agonist therapy and asthma mortality in Japan. *Lancet* **351**:1406–1407 (1998).
- H. Foth. Role of the lung in accumulation and metabolism of xenobiotic compounds—implications for chemically induced toxicity. *Crit. Rev. Toxicol.* **25**:165–205 (1995).
- M. Takano, K. Inui, T. Okano, H. Saito, and R. Hori. Carrier-mediated transport systems of tetraethylammonium in rat renal brush-border and basolateral membrane vesicles. *Biochim. Biophys. Acta* **773**:113–124 (1984).
- J. K. Chun, L. Zhang, M. Piquette-Miller, E. Lau, L. Q. Tong, and K. M. Giacomini. Characterization of guanidine transport in human renal brush border membranes. *Pharm. Res.* **14**:936–941 (1997).
- R. H. Moseley and R. W. van Dyke. Organic cation transport by rat liver lysosomes. *Am. J. Physiol.* **268**:G480–G486 (1995).
- M. T. Whittico, G. Yuan, and K. M. Giacomini. Cimetidine transport in isolated brush border membrane vesicles from bovine choroid plexus. *J. Pharmacol. Exp. Ther.* **255**:615–623 (1990).
- S. Zevin, M. E. Schaner, N. P. Illsley, and K. M. Giacomini. Guanidine transport in a human choriocarcinoma cell line (JAR). *Pharm. Res.* **14**:401–405 (1997).
- Y. Miyamoto, V. Ganapathy, and F. H. Leibach. Transport of guanidine in rabbit intestinal brush-border membrane vesicles. *Am. J. Physiol.* **255**:G85–G92 (1988).
- J. M. Cheek, K. J. Kim, and E. D. Crandall. Tight monolayer of rat alveolar epithelial cells: bioelectric properties and active sodium transport. *Am. J. Physiol.* **256**:C668–C693 (1989).
- M. M. Berg, K.-J. Kim, R. L. Lubman, and E. D. Crandall. Hydrophilic solute transport across rat alveolar epithelium. *J. Appl. Physiol.* **66**:2320–2327 (1989).
- R. J. Mason, S. R. Walker, B. A. Shields, J. E. Henson, and M. C. Williams. Identification of rat alveolar type II epithelial cells with a tannic acid and polychrome stain. *Am. Rev. Respir. Dis.* **131**:786–788 (1985).
- R. H. Simon, J. P. McCoy, A. E. Chu, P. D. Dehart, and I. J. Goldstein. Binding of *Griffonia simplicifolia* I lectin to rat pulmonary alveolar macrophages and its use in purifying type II alveolar epithelial cells. *Biochim. Biophys. Acta* **885**:34–42 (1986).
- J. D. Edelson, J. M. Shannon, and R. J. Mason. Alkaline phosphatase: a marker of alveolar type II cell differentiation. *Am. Rev. Respir. Dis.* **138**:1268–1275 (1988).
- T. W. Robison and K. J. Kim. Air-interface cultures of guinea pig airway epithelial cells: effects of active  $\text{Na}^+$  and  $\text{Cl}^-$  transport inhibitors on bioelectric properties. *Exp. Lung Res.* **20**:101–117 (1994).
- H. Koepsell. Organic cation transporters in intestine, kidney, liver, and brain. *Ann. Rev. Physiol.* **60**:243–266 (1998).
- J. M. Cheek, M. J. Evans, and E. D. Crandall. Type-I cell-like morphology in tight alveolar epithelial monolayers. *Exp. Cell Res.* **184**:375–387 (1989).
- K. J. Elbert, U. F. Schäfer, H.-J. Schäfers, K. J. Kim, V. H. L. Lee, and C.-M. Lehr. Monolayers of human alveolar epithelial cells in primary culture for pulmonary absorption and transport studies. *Pharm. Res.* **16**:601–608 (1999).
- B. Goodman, K.-J. Kim, and E. D. Crandall. Evidence for active sodium transport across alveolar epithelium of isolated rat lung. *J. Appl. Physiol.* **62**:703–710 (1987).
- V. G. Nielsen, M. D. Duvall, M. S. Baird, and S. Matalon. cAMP activation of chloride and fluid secretion across the rabbit alveolar epithelium. *Am. J. Physiol.* **275**:L1127–L1133 (1998).
- K. J. Kim, J. M. Cheek, and E. D. Crandall. Contribution of active  $\text{Na}^+$  and  $\text{Cl}^-$  fluxes to net ion transport by alveolar epithelium. *Respir. Physiol.* **85**:245–256 (1991).
- P. P. Sokol and T. D. McKinney. Mechanisms of organic cation transport in rabbit renal basolateral membrane vesicles. *Am. J. Physiol.* **258**:F1599–F1607 (1990).

28. S. H. Wright. Transport of N<sub>1</sub>-methylnicotinamide across brush border membrane vesicles from rabbit kidney. *Am. J. Physiol.* **249**:F903–F911 (1985).
29. D. Gründemann, J. Babin-Ebell, F. Martel, N. Örding, A. Schmidt, and E. Schömig. Primary structure and functional expression of the apical organic cation transporter from kidney epithelial LLC-PK<sub>1</sub> cells. *J. Biol. Chem.* **272**:10408–10413 (1997).
30. D. E. Rannels, A. E. Pegg, R. S. Clark, and J. L. Addison. Interaction of paraquat and amine uptake by rat lungs perfused *in situ*. *Am. J. Physiol.* **249**:E506–E513 (1985).